Various flow amplitudes in 2D non-Oberbeck-Boussinesq Rayleigh-Bénard convection in water

Enrico Calzavarini[1], Siegfried Grossmann[2*], Detlef Lohse[1], and Kazuyasu Sugiyama[1]

[1] Physics of Fluids group, Department of Applied Physics, J. M. Burgers Centre for Fluid Dynamics, and Impact-, MESA-, and BMTI-Institutes, University of Twente, P. O. Box 217, 7500 AE Enschede, The Netherlands,
[2] Fachbereich Physik, Philipps-Universität Marburg, 35032 Marburg, Germany,
*grossmann at physik.uni-marburg.de

The flow organization in Rayleigh-Bénard turbulence including Non-Oberbeck-Boussinesq (NOB) effects is numerically analyzed. The working fluid is water, the aspect ratio is $\Gamma = 1$, and we restrict ourselves to two-dimensional flow. We focus here on a summary of the structure of the velocity field. A more detailed analysis of the flow structure as well as on the temperature profiles, the center temperature and the Nusselt number is given in [1].

The thermal flow develops several large scale coherent structures and thus has to be described by several velocity amplitudes (or Reynolds numbers). These include the volume and time averaged energy based velocity amplitude

$$Re^E = \left\langle \frac{1}{2}\mathbf{u}^2 \right\rangle_{V,\tau}^{1/2} \cdot L/\nu, \tag{1}$$

and local wind amplitudes $Re(x_j) = \left\langle \frac{1}{2}\mathbf{u}^2(x_j) \right\rangle_{\tau}^{1/2} \cdot L/\nu$ for certain characteristic positions x_j, e.g. in the cell center, at the profiles' maxima, in the corner rolls etc. Correspondingly, one also has to introduce and study several velocity profiles, area averaged or local ones. These together describe the various features of the rather complex flow organization.

Our results for the center temperature T_c are presented both as functions of the Rayleigh number Ra (with Ra up to 10^8) for fixed temperature difference Δ between top and bottom plates and as functions of Δ (which measures the "non-Oberbeck-Boussinesqness") for fixed Ra with Δ up to 60K (see Figure 1). All results are consistent with the available experimental NOB data for the center temperature T_c and the Nusselt number ratio Nu_{NOB}/Nu_{OB}. Here, the labels OB and NOB mean that the Oberbeck-Boussinesq conditions are either valid or are not guaranteed any more, respectively, i.e., $Nu_{NOB} \equiv Nu$ is the actually measured Nusselt number.

B. Eckhardt (ed.), *Advances in Turbulence XII*, Springer Proceedings in Physics 132,
DOI 10.1007/978-3-642-03085-7_114,

For the temperature profiles we find – due to plume emission from the boundary layers – increasing deviations from the extended Prandtl-Blasius boundary layer theory presented in [2] with increasing Ra, while the center temperature itself is surprisingly well predicted by that theory.

For given non-Oberbeck-Boussinesqness Δ both the center temperature T_c and the Nusselt number ratio Nu_{NOB}/Nu_{OB} only weakly depend on Ra.

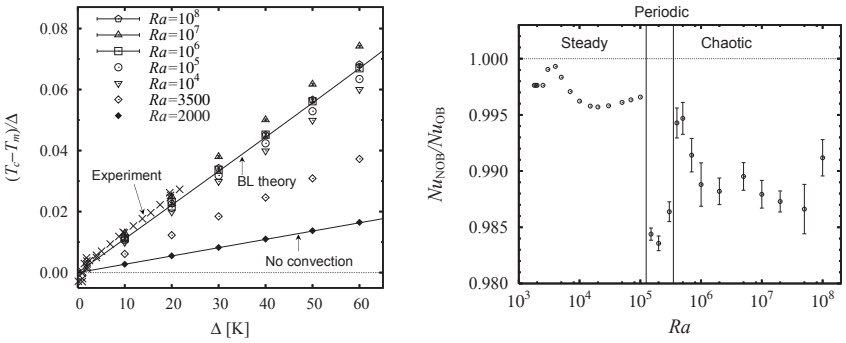

Fig. 1. Left: Relative deviation $(T_c - T_m)/\Delta$ of the horizontally area (and time) averaged center temperature T_c from the arithmetic mean temperature T_m in terms of Δ versus the temperature difference Δ for water at fixed $T_m = 40^o$C for various values of Ra. Right: Nusselt number ratio Nu_{NOB}/Nu_{OB} vs. Rayleigh number Ra for water at fixed values for $T_m = 40^o$C and $\Delta = 40$K. It is also indicated where the state is steady, periodic, or chaotic. Apparently there is a tiny reduction of the heat flux Nu due to deviations from Oberbeck-Boussinesq conditions, about 1% or so.

Concerning the flow structure we find that beyond $Ra \approx 10^6$ the flow consists of a large diagonal center convection roll and two smaller rolls in the upper and lower corners, respectively ("corner flows"), see Figure 2. In the NOB case the center convection roll is still characterized by only one velocity scale. In contrast, the top and bottom corner flows are then of different strengths, the velocity amplitude of the bottom corner roll being a factor 1.3 larger (for $\Delta = 40$K) than the top one. We attribute this to the lower viscosity in the hotter bottom boundary layer.

Under OB-conditions we find a scaling of the volume averaged energy based velocity amplitude as $Re^E_{OB} \propto Ra^\gamma$ with an exponent $\gamma = 0.62$. As the NOBness increases, the enhanced lower corner flow as well as the enhanced center roll lead to an enhancement of the energy based Reynolds number Re^E of about 4% to 5% for $\Delta = 60$K. Trying to understand this we consider the free fall velocity of fluid elements in thermal concetion $v \propto \sqrt{\beta g L \Delta}$, leading to $Re^E_{NOB}/Re^E_{OB} \propto (\beta(T_c)/\beta(T_m))^{0.5}$. Here $\beta(T)$ is the thermal expansion coefficient, taken either at the center T_c or the arithmetic mean temperature T_m between top and bottom plate temperatures. The β-ratio as a function of

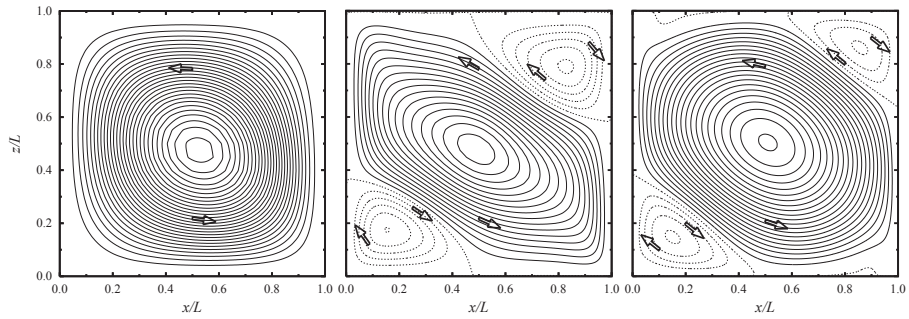

Fig. 2. Lines of constant values for the conditionally time averaged velocity field $\bar{\mathbf{u}}(x,z)$ at different Rayleigh numbers $Ra = 10^4, 10^6, 10^8$ in Rayleigh-Bénard convection. (Conditional time averaging takes the time dependent rotational direction of the wind into account.) Counterclockwise velocity direction (as indicated by arrows) is drawn with solid lines, while the clockwise ones are indicated by dotted lines. The OB flow structure, which already develops secondary (counter) rolls enjoys top-bottom symmetry, which is broken for the shown NOB case. There are major secondary rolls only in those corners, where the downcoming or the upgoing wind is directed towards the bottom or top plates, respectively.

the NOBness is included in Figure 3 a. It seems to be consistent with the numerical Reynolds number data, also in their dependence on Ra. - To support this, we artificially switched off the temperature dependence of β in the numerics. Then the NOB modifications of Re^E is less than 1% even at $\Delta = 60$K, revealing the temperature dependence of the thermal expansion coefficient as the main origin of the NOB effects on the global Reynolds number in water.

The found ratio-relation might suggest that the NOB Reynolds number can be related to the OB one by simply allowing for the temperature variation of $\beta(T)$ due to the NOB-shift of $T_m \to T_c$ in the Rayleigh number, keeping the other material parameters at their fixed values ν_m, κ_m. One then has $\tilde{Re}^E_{NOB} \propto (\beta(T_c) g L^3 \Delta/\nu_m\kappa_m)^{0.62} = (\beta(T_c)/\beta(T_m)^{0.62} \cdot Ra_m^{0.62} \propto (\beta(T_c)/\beta(T_m))^{0.62} \cdot Re_{OB}$. This leads to an analogous Re^E and β ratio relation as before, but with the numerical exponent 0.62 (Figure 3 (b)). For larger Ra the ratio $(\beta(T_c)/\beta(T_m)^{0.62}$ is even closer to the numerical Re^E_{NOB}/Re^E_{OB} data. - But note that $\beta(T) g L^3 \Delta/\nu_m\kappa_m$ no longer is the physical control parameter!

Of interest are also the various flow profiles, e.g. the area averaged velocity amplitudes $U_x(z)$ as a function of height $0 \le z/L \le 1$ as well as the side wall wind $U_z(x)$ as a function of the wall distance $0 \le x/L \le 1$. These amplitudes are defined as $U_x(z) = \langle\overline{u_x}\rangle_{x(z)}(z)$ and $U_z(x) = \langle\overline{u_z}\rangle_{z(x)}(x)$, where the overline denotes the time average and $\langle ...\rangle$ indicates averaging along the x-direction for fixed z etc. In Figure 4 we summarize one of our profile results.

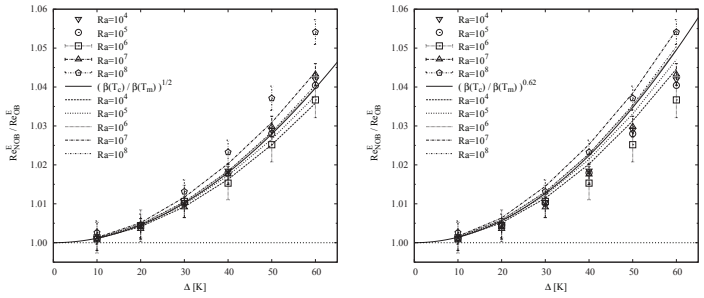

Fig. 3. NOB effect on the Reynolds number ratio Re^E_{NOB}/Re^E_{OB} as function of the NOBness Δ, compared with $(\beta_c/\beta_m)^\gamma$. Left: $\gamma = 1/2$, according to free fall velocity; right: $\gamma = 0.62$. Apparently, it is the NOB deviation of $T_m \to T_c$ in the expansion coefficient which is the main NOB effect on the wind amplitude.

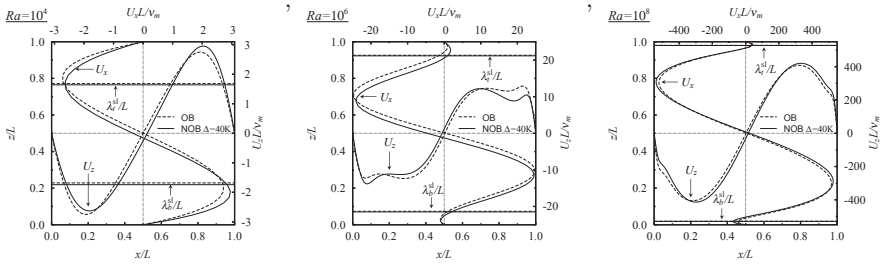

Fig. 4. The vertical and horizontal velocity profiles $U_x(z)$ and $U_z(x)$ as derived from the conditionally time averaged velocity components $\overline{u_x}$ and $\overline{u_z}$ at three different Ra numbers $10^4, 10^6, 10^8$. The abscissa and ordinate scales are the dimensionless width and height. The upper scales show the horizontal velocity profiles nondimensionalized with ν_m/L, i.e., $Re_x(z)$; the right scales show the vertical velocity's $U_z(x)$ profiles, also nondimensionalized by ν_m/L. Dashed lines indicate the OB case, full lines NOB case. In both cases $\Delta = 40$K. Also indicated are the corresponding thermal slope BL widths $\lambda^{sl}_{b,t}$, which strongly decrease with increasing Ra.

References

1. Kazuyasu Sugiyama, Enrico Calzavarini, Siegfried Grossmann, and Detlef Lohse, *Flow organization in non-Oberbeck-Boussinesq Rayleigh-Bénard convection in water*, accepted in JFM, 2009.
2. Guenter Ahlers, Eric Brown, Francisco Fontenele Araujo, Denis Funfschilling, Siegfried Grossmann, and Detlef Lohse, J. Fluid Mech. 569, 409 - 445 (2006).